

# RSC Advances



This is an *Accepted Manuscript*, which has been through the Royal Society of Chemistry peer review process and has been accepted for publication.

*Accepted Manuscripts* are published online shortly after acceptance, before technical editing, formatting and proof reading. Using this free service, authors can make their results available to the community, in citable form, before we publish the edited article. This *Accepted Manuscript* will be replaced by the edited, formatted and paginated article as soon as this is available.

You can find more information about *Accepted Manuscripts* in the [Information for Authors](#).

Please note that technical editing may introduce minor changes to the text and/or graphics, which may alter content. The journal's standard [Terms & Conditions](#) and the [Ethical guidelines](#) still apply. In no event shall the Royal Society of Chemistry be held responsible for any errors or omissions in this *Accepted Manuscript* or any consequences arising from the use of any information it contains.

**Multiple target chemosensor: a fluorescent sensor for Zn(II) and Al(III) and chromogenic sensor for Fe(II) and Fe(III)**

Yong Sung Kim, Gyeong Jin Park, Jae Jun Lee, Sun Young Lee, Seong Youl Lee, Cheal Kim\*

<sup>a</sup> Department of Fine Chemistry and Department of Interdisciplinary Bio IT Materials, Seoul National University of Science and Technology, Seoul 139-743, Korea. Fax: +82-2-973-9149; Tel: +82-2-970-6693; E-mail: chealkim@seoultech.ac.kr

**Abstract**

A multifunctional fluorescent and colorimetric chemosensor **1**, based on two julolidine moieties as a binding and signaling unit, has been synthesized in a one-step procedure. Receptor **1** showed prompt responses toward Zn<sup>2+</sup> and Al<sup>3+</sup> ions through selective fluorescence enhancement in dimethylformamide (DMF), while the presence of 5% water rendered **1** detect only Zn<sup>2+</sup>. Moreover, **1** sensed the iron by “naked eye” with the clear color change. Upon the addition of Fe<sup>2+</sup> and Fe<sup>3+</sup> into each solution of **1**, the color of the solutions changed from pale yellow to dark green for both Fe<sup>2+</sup> and Fe<sup>3+</sup>. The binding modes of the complexes were determined to be 1:1 complexation stoichiometry through Job plot, <sup>1</sup>H NMR titration and ESI-mass spectrometry analysis.

**Keywords:** Multiple analytes; Chromogenic; Fluorescent; Schiff base; Sensor

## Introduction

As the second most abundant transition metal ion in the human body, zinc ion ( $\text{Zn}^{2+}$ ) plays an important role in gene transcription, regulation of metalloenzymes, neural signal transmission and apoptosis.<sup>1-11</sup> However, the imbalance in zinc may cause several health problem including superficial skin disease, prostate cancer, diabetes, and brain diseases such as Alzheimer's disease, Friedreich's ataxia, and Parkinson's disease.<sup>12-19</sup> Therefore, it is very significant to efficiently detect zinc ion. Nevertheless, many of the reported  $\text{Zn}^{2+}$  sensors suffer from a limited choice of the spectroscopic instruments due to its inherent  $d^{10}$  shell, insufficient selectivity or sensitivity, and interference from other transition metal ions, especially cadmium ion, which is in the same group of the periodic table and shows similar properties to zinc ion.<sup>20-21</sup>

Aluminum is the most abundant (8.3 % by weight) metallic element and the third most abundant of all elements (after oxygen and silicon) in the earth's crust.<sup>22</sup> Compounds of aluminum are widely dispersed in various ways; textile industry, medicines (antacids), bleached flour, paper industry, food additives, aluminum-based pharmaceuticals, storage/cooking utensils, and production of light alloys.<sup>23-27</sup> However, high amounts of aluminum ion are not only harmful to plant growth but also damage the human nervous system to induce Alzheimer's disease, Parkinson's disease, and amyotrophic lateral sclerosis.<sup>28-31</sup> Thus, the development of chemo-sensor for aluminum ( $\text{Al}^{3+}$ ) still progresses with a considerable attention. Nevertheless, the detection of  $\text{Al}^{3+}$  is difficult because of the lack of spectroscopic characteristics and poor coordination ability comparing other transition metals. Therefore, the development of new sensors for  $\text{Al}^{3+}$  with high selectivity is more required for environment and biological fields.<sup>32</sup>

Iron is the most abundant transition metal for both plants and animals. It plays an important role in cellular metabolism, enzyme catalysis, and, as an oxygen carrier in hemoglobin and a cofactor in many enzymatic reactions.<sup>33-35</sup> However, less iron in the body has been reported linked to diabetes, anemia, liver and kidney damages, and heart diseases.<sup>36</sup> Accordingly, the development of methods to detect iron in environment and biological fields is of considerable significance.<sup>37</sup>

For these reasons, development of chemosensors for the detection of these metal ions ( $\text{Zn}^{2+}$ ,  $\text{Al}^{3+}$ ,  $\text{Fe}^{2+}$ , and  $\text{Fe}^{3+}$ ) has been considered as a greatly worthy research. Moreover, single

probes for multiple targets are being actively considered due to the benefits such as less expensive and efficient analysis, while most chemosensors developed to date are based on single-ion responsive systems.<sup>38-42</sup>

Herein, we report on development and application of chemosensor **1** for multiple analytes based on the julolidine moiety well-known as a good fluorophore and chromophore.<sup>43-45</sup> **1** detected effectively the most abundant and fundamental ions ( $\text{Zn}^{2+}$ ,  $\text{Al}^{3+}$ ,  $\text{Fe}^{2+/3+}$ ) in the ecosystem through two different sensing mechanisms (fluorescent and colorimetric responses).

## Experimental Section

### Materials and Instrumentation

All the starting materials (analytical grade and spectroscopic grade) for synthesis were commercially available and used as received.  $^1\text{H}$  NMR and  $^{13}\text{C}$  NMR measurements were performed on a Varian 400 MHz spectrometer and chemical shifts are recorded in ppm. Electrospray ionization mass spectra (ESI-MS) were collected on a Thermo Finnigan (San Jose, CA, USA) LCQTM Advantage MAX quadrupole ion trap instrument. Elemental analysis for carbon, nitrogen, and hydrogen was carried out by using a Flash EA 1112 elemental analyzer (thermo) in Organic Chemistry Research Center of Sogang University, Korea. Absorption spectra were recorded at room temperature using a Perkin Elmer model Lambda 2S UV/Vis spectrometer. Fluorescence measurements were performed on a Perkin Elmer model LS45 fluorescence spectrometer.

### Synthesis of **1**

A solution of 8-hydroxyjulolidine-9-carboxaldehyde (0.69 g, 3.04 mmol) in ethanol was added to a solution containing 2, 2'-thiobis(ethylamine) (199  $\mu\text{L}$ , 1.60 mmol) in ethanol. The reaction mixture was stirred for 12 h at room temperature. After evaporation, the product was recrystallized by ether, filtered, and dried under vacuum. The yield: 0.47 g (59.6 %).  $^1\text{H}$  NMR (400 MHz,  $\text{CDCl}_3$ )  $\delta$  (ppm): 13.75 (s, 2H), 7.93 (s, 2H), 6.59 (s, 2H), 3.64 (t,  $J = 6.8$  Hz, 4H), 3.22-3.16 (m, 8H), 2.81-2.77 (t,  $J = 6.8$  Hz, 4H), 2.70 (t,  $J = 6.6$  Hz, 4H), 2.65 (t,  $J =$

6.2 Hz 4H), 1.96-1.89 (m, 8H),  $^{13}\text{C}$  NMR ( $\text{CDCl}_3$ , 400 MHz):  $\delta$  165.40, 160.46, 146.59, 129.54, 112.22, 107.87, 106.34, 57.37, 50.00, 49.62, 33.44, 27.35, 22.32, 21.38, 20.79 ppm. LRMS (ESI)  $m/z$   $[\text{M}+\text{H}^+]$ : calcd, 519.279; found, 519.267. Anal. Calcd for  $\text{C}_{30}\text{H}_{38}\text{N}_4\text{O}_2\text{S}$  (518.272): C, 69.46; H, 7.38; N, 10.80. Found: C, 69.39; H, 7.63; N, 10.54 %.

### Fluorescence chemosensor

**Fluorescence titrations.** For  $\text{Zn}^{2+}$  ion in DMF; **1** (3.1 mg, 0.003 mmol) was dissolved in DMF (2 mL). 10  $\mu\text{L}$  of **1** (3 mM) were diluted in 2.990 mL DMF to make the final concentration of 10  $\mu\text{M}$ .  $\text{Zn}(\text{NO}_3)_2$  (18.2 mg, 0.02 mmol) were dissolved in DMF (3 mL). 1.5-16.5  $\mu\text{L}$  of the  $\text{Zn}(\text{NO}_3)_2$  solution (20 mM) were transferred to the receptor solution (10  $\mu\text{M}$ ) prepared above. After mixing them for two minutes, fluorescence spectra were taken at room temperature.

For  $\text{Al}^{3+}$  ion in DMF; **1** (3.1 mg, 0.003 mmol) was dissolved in DMF (2 mL). 10  $\mu\text{L}$  of **1** (3 mM) were diluted in 2.990 mL DMF to make the final concentration of 10  $\mu\text{M}$ .  $\text{Al}(\text{NO}_3)_3$  (22.5 mg, 0.02 mmol) were dissolved in DMF (3 mL). 1.5-16.5  $\mu\text{L}$  of the  $\text{Al}(\text{NO}_3)_3$  solution (20 mM) were transferred to the receptor solution (10  $\mu\text{M}$ ) prepared above. After mixing them for two minutes, fluorescence spectra were taken at room temperature.

For  $\text{Zn}^{2+}$  ion in aqueous media; **1** (3.1 mg, 0.003 mmol) was dissolved in DMF (2 mL). The receptor solution (10  $\mu\text{L}$ , 3 mM) was diluted in 2.990 mL DMF-buffer solution (95:5, v/v, 10 mM, bis-tris, pH 7.0) to make the final concentration of 10  $\mu\text{M}$ .  $\text{Zn}(\text{NO}_3)_2$  (18.2 mg, 0.02 mmol) was dissolved in DMF (3 mL). 1.5-18.0  $\mu\text{L}$  of the  $\text{Zn}(\text{NO}_3)_2$  solution (20 mM) were transferred to each receptor solution (10  $\mu\text{M}$ ) prepared above. After mixing them for two minutes, fluorescence spectra were taken at room temperature.

**UV-vis titrations.** For  $\text{Zn}^{2+}$  ion in DMF; Receptor **1** (3.1 mg, 0.003 mmol) was dissolved in DMF (2 mL). 10  $\mu\text{L}$  of **1** (3 mM) were diluted with 2.990 mL DMF to make the final concentration of 10  $\mu\text{M}$ .  $\text{Zn}(\text{NO}_3)_2$  (18.2 mg, 0.02 mmol) were dissolved in DMF (3 mL). 0.3-2.7  $\mu\text{L}$  of the  $\text{Zn}(\text{NO}_3)_2$  solution (20 mM) were transferred to the receptor solution (10  $\mu\text{M}$ ) prepared above. After mixing them for two minutes, UV-vis absorption spectra were

taken at room temperature.

For  $\text{Al}^{3+}$  ion in DMF; **1** (3.1 mg, 0.003 mmol) was dissolved in DMF (2 mL). 10  $\mu\text{L}$  of **1** (3 mM) were diluted with 2.990 mL DMF to make the final concentration of 10  $\mu\text{M}$ .  $\text{Al}(\text{NO}_3)_3$  (22.5 mg, 0.02 mmol) were dissolved in DMF (3 mL). 0.75-6.0  $\mu\text{L}$  of the  $\text{Al}(\text{NO}_3)_3$  solution (20 mM) were transferred to the receptor solution (10  $\mu\text{M}$ ) prepared above. After mixing them for two minutes, UV-vis absorption spectra were taken at room temperature

For  $\text{Zn}^{2+}$  ion in aqueous media; **1** (3.1 mg, 0.003 mmol) was dissolved in DMF (2 mL). 10  $\mu\text{L}$  of **1** (3 mM) were diluted with 2.990 mL in DMF-buffer solution (95:5, v/v, 10 mM, bis-tris, pH 7.0) to make the final concentration of 10  $\mu\text{M}$ .  $\text{Zn}(\text{NO}_3)_2$  (18.2 mg, 0.02 mmol) were dissolved in DMF (3 mL). 0.75-6.0  $\mu\text{L}$  of the  $\text{Zn}(\text{NO}_3)_2$  solution (20 mM) were transferred to the receptor solution (10  $\mu\text{M}$ ) prepared above. After mixing them for two minutes, UV-vis absorption spectra were taken at room temperature.

**Competition with other metal ions.** For  $\text{Zn}^{2+}$  ion in DMF; Receptor **1** (3.1 mg, 0.003 mmol) was dissolved in DMF (2 mL). 10  $\mu\text{L}$  of **1** (3 mM) were diluted with 2.990 mL DMF to make the final concentration of 10  $\mu\text{M}$ .  $\text{MNO}_3$  ( $\text{M} = \text{Na}, \text{K}$ , 0.02 mmol),  $\text{M}(\text{NO}_3)_2$  ( $\text{M} = \text{Mg}, \text{Ca}, \text{Mn}, \text{Ni}, \text{Cu}, \text{Zn}, \text{Cd}, \text{Hg}$ , 0.02 mmol),  $\text{M}(\text{NO}_3)_3$  ( $\text{M} = \text{Al}, \text{Cr}, \text{Fe}, \text{Ga}, \text{In}$ , 0.02 mmol) and  $\text{Fe}(\text{ClO}_4)_2$  (15.6 mg, 0.02 mmol) were dissolved in DMF (3 mL), respectively. 16.5  $\mu\text{L}$  of each metal solution (20 mM) were taken and added into 3 mL of each receptor solution (10  $\mu\text{M}$ ) prepared above to make 11 equiv. Then, 16.5  $\mu\text{L}$  of  $\text{Zn}(\text{NO}_3)_2$  solution (20 mM) were added into the mixed solution of each metal ion and **1** to make 11 equiv. After mixing them for two minutes, fluorescence spectra were taken at room temperature.

For  $\text{Al}^{3+}$  ion in DMF; **1** (3.1 mg, 0.003 mmol) was dissolved in DMF (2 mL). 10  $\mu\text{L}$  of **1** (3 mM) were diluted with 2.990 mL DMF to make the final concentration of 10  $\mu\text{M}$ .  $\text{MNO}_3$  ( $\text{M} = \text{Na}, \text{K}$ , 0.02 mmol),  $\text{M}(\text{NO}_3)_2$  ( $\text{M} = \text{Mg}, \text{Ca}, \text{Mn}, \text{Ni}, \text{Cu}, \text{Zn}, \text{Cd}, \text{Hg}$ , 0.02 mmol),  $\text{M}(\text{NO}_3)_3$  ( $\text{M} = \text{Al}, \text{Cr}, \text{Fe}, \text{Ga}, \text{In}$ , 0.02 mmol) and  $\text{Fe}(\text{ClO}_4)_2$  (15.6 mg, 0.02 mmol) were dissolved in DMF (3 mL), respectively. 16.5  $\mu\text{L}$  of each metal solution (20 mM) were taken and added into 3 mL of each receptor solution (10  $\mu\text{M}$ ) prepared above to make 11 equiv. Then, 16.5  $\mu\text{L}$  of  $\text{Al}(\text{NO}_3)_3$  solution (20 mM) were added into the mixed solution of each metal ion and **1** to make 11 equiv. After mixing them for two minutes, fluorescence spectra were taken at room temperature.

For  $\text{Zn}^{2+}$  ion in aqueous media; **1** (3.1 mg, 0.003 mmol) was dissolved in DMF (2 mL). 10  $\mu\text{L}$  of **1** (3 mM) were diluted with 2.990 mL in DMF-buffer solution (95:5, v/v, 10 mM, bis-tris, pH 7.0) to make the final concentration of 10  $\mu\text{M}$ .  $\text{MNO}_3$  (M = Na, K, 0.02 mmol),  $\text{M}(\text{NO}_3)_2$  (M = Mg, Ca, Mn, Ni, Cu, Zn, Cd, Hg, 0.02 mmol),  $\text{M}(\text{NO}_3)_3$  (M = Al, Cr, Fe, Ga, In, 0.02 mmol) and  $\text{Fe}(\text{ClO}_4)_2$  (15.6 mg, 0.02 mmol) were dissolved in DMF (3 mL), respectively. 18  $\mu\text{L}$  of each metal solution (20 mM) were taken and added into 3 mL of each receptor solution (10  $\mu\text{M}$ ) prepared above to make 12 equiv. Then, 18  $\mu\text{L}$  of  $\text{Zn}(\text{NO}_3)_2$  solution (20 mM) were added into the mixed solution of each metal ion and **1** to make 12 equiv. After mixing them for two minutes, fluorescence spectra were taken at room temperature.

**Job plot measurements.** For  $\text{Zn}^{2+}$  ion in DMF; Receptor **1** (3.1 mg, 0.003 mmol) was dissolved in DMF (2 mL). 100, 90, 80, 70, 60, 50, 40, 30, 20, 10 and 0  $\mu\text{L}$  of **1** solution were taken and transferred to vials. Each vial was diluted with DMF to make a total volume of 2.9 mL.  $\text{Zn}(\text{NO}_3)_2$  (2.7 mg, 0.003 mmol) was dissolved in DMF (3 mL). 0, 10, 20, 30, 40, 50, 60, 70, 80, 90, and 100  $\mu\text{L}$  of the  $\text{Zn}^{2+}$  solution were added to each diluted **1** solution. Each vial had a total volume of 3 mL. After shaking them for two minutes, fluorescence spectra were taken at room temperature.

For  $\text{Al}^{3+}$  ion in DMF; **1** (3.1 mg, 0.003 mmol) was dissolved in DMF (2 mL). 100, 90, 80, 70, 60, 50, 40, 30, 20, 10 and 0  $\mu\text{L}$  of the **1** solution were taken and transferred to vials. Each vial was diluted with DMF to make a total volume of 2.9 mL.  $\text{Al}(\text{NO}_3)_3$  (3.4 mg, 0.003 mmol) was dissolved in DMF (3 mL). 0, 10, 20, 30, 40, 50, 60, 70, 80, 90, and 100  $\mu\text{L}$  of the  $\text{Al}^{3+}$  solution were added to each diluted **1** solution. Each vial had a total volume of 3 mL. After shaking them for two minutes, fluorescence spectra were taken at room temperature.

For  $\text{Zn}^{2+}$  ion in aqueous media; **1** (3.1 mg, 0.003 mmol) was dissolved in DMF. 100, 90, 80, 70, 60, 50, 40, 30, 20, 10 and 0  $\mu\text{L}$  of the **1** solution were taken and transferred to vials. Each vial was diluted with DMF-buffer solution (95:5, v/v, 10 mM, bis-tris, pH 7.0) to make a total volume of 2.9 mL.  $\text{Zn}(\text{NO}_3)_2$  (2.7 mg, 0.003 mmol) was dissolved in DMF (3 mL). 0, 10, 20, 30, 40, 50, 60, 70, 80, 90, and 100  $\mu\text{L}$  of the  $\text{Zn}^{2+}$  solution were added to each diluted **1** solution. Each vial had a total volume of 3 mL. After shaking them for two minutes, fluorescence spectra were taken at room temperature.

**NMR titrations.** For  $^1\text{H}$  NMR titrations of receptor **1** with zinc ion, three NMR tubes of **1** (3.2 mg, 0.01 mmol) dissolved in  $\text{DMF-}d_7$  (700  $\mu\text{L}$ ) were prepared and then three different equiv (0, 0.5 and 1 equiv) of  $\text{Zn}(\text{NO}_3)_2 \cdot 6\text{H}_2\text{O}$  dissolved in DMF were added to each solution of **1**. After shaking them for two minutes,  $^1\text{H}$  NMR spectra were taken at room temperature.

For  $^1\text{H}$  NMR titrations of **1** with aluminium ion, three NMR tubes of **1** (3.2 mg, 0.01 mmol) dissolved in  $\text{DMF-}d_7$  (700  $\mu\text{L}$ ) were prepared and three different concentrations (0, 0.6 and 1 equiv) of  $\text{Al}(\text{NO}_3)_3 \cdot 6\text{H}_2\text{O}$  dissolved in DMF were added to each solution of **1**. After shaking them for two minutes,  $^1\text{H}$  NMR spectra were taken at room temperature.

**Reversible test.** Receptor **1** (3.1 mg, 0.003 mmol) was dissolved in DMF (2 mL) and 10  $\mu\text{L}$  (3 mM) of it were diluted with 2.990 mL DMF-buffer solution (95:5, v/v, 10 mM, bis-tris, pH 7.0) to make a final concentration of 10  $\mu\text{M}$ .  $\text{Zn}(\text{NO}_3)_2 \cdot 5\text{H}_2\text{O}$  (18.2 mg, 0.02 mmol) was dissolved in DMF (3 mL) and 18  $\mu\text{L}$  of the  $\text{Zn}^{2+}$  ion solution (20 mM) were added to the solution of **1** (10  $\mu\text{M}$ ) prepared above. After mixing it for two minutes, fluorescence spectrum was taken at room temperature. Ethylenediaminetetraacetic acid disodium salt dehydrate (EDTA, 0.4 mmol) was dissolved in buffer solution (5 mL) and 9  $\mu\text{L}$  of the EDTA solution (40 mM) were added to the solution of **1**- $\text{Zn}^{2+}$  complex (10  $\mu\text{M}$ ) prepared above. After mixing it for two minutes, fluorescence spectrum was taken. For the reversibility study, 18  $\mu\text{L}$  of the  $\text{Zn}^{2+}$  ion solution (20 mM) was added to the above solution. After mixing it for two minutes, fluorescence spectrum was taken at room temperature.

### Colormetric chemosensor

**UV-Vis titrations.** For  $\text{Fe}^{2+}$ ; Receptor **1** (3.1 mg, 0.003 mmol) was dissolved in MeOH (2 mL). 10  $\mu\text{L}$  of **1** (3 mM) were diluted with 2.990 mL in MeOH-buffer solution (9:1, v/v, 10 mM, bis-tris, pH 7.0) to make the final concentration of 10  $\mu\text{M}$ .  $\text{Fe}(\text{ClO}_4)_2$  (15.6 mg, 0.02 mmol) were dissolved in MeOH (3 mL). 0.3-3.0  $\mu\text{L}$  of the  $\text{Fe}(\text{ClO}_4)_2$  solution (20 mM) were transferred to the receptor solution (10  $\mu\text{M}$ ) prepared above. After mixing them for two minutes, UV-vis absorption spectra were taken at room temperature.

For  $\text{Fe}^{3+}$  ion; **1** (3.1 mg, 0.003 mmol) was dissolved in MeOH. 10  $\mu\text{L}$  of **1** (3 mM) were

diluted with 2.990 mL MeOH-buffer solution (9:1, v/v, 10 mM, bis-tris, pH 7.0) to make the final concentration of 10  $\mu\text{M}$ .  $\text{Fe}(\text{NO}_3)_3$  (24.7 mg, 0.02 mmol) were dissolved in MeOH (3 mL). 0.3-1.65  $\mu\text{L}$  of the  $\text{Fe}(\text{NO}_3)_3$  solution (20 mM) were transferred to the receptor solution (10  $\mu\text{M}$ ) prepared above. After mixing them for two minutes, UV-vis absorption spectra were taken at room temperature.

**Competition with other metal ions.** For  $\text{Fe}^{2+}$  ion; Receptor **1** (3.1 mg, 0.003 mmol) was dissolved in MeOH (2 mL). 10  $\mu\text{L}$  of **1** (3 mM) were diluted with 2.990 mL MeOH-buffer solution (9:1, v/v, 10 mM, bis-tris, pH 7.0) to make the final concentration of 10  $\mu\text{M}$ .  $\text{MNO}_3$  (M = Na, K, 0.02 mmol),  $\text{M}(\text{NO}_3)_2$  (M = Mg, Ca, Mn, Ni, Cu, Zn, Cd, Hg, 0.02 mmol),  $\text{M}(\text{NO}_3)_3$  (M = Al, Cr, Fe, Ga, In, 0.02 mmol) and  $\text{Fe}(\text{ClO}_4)_2$  (15.6 mg, 0.02 mmol) were dissolved in MeOH (3 mL), respectively. 3.0  $\mu\text{L}$  of each metal solution (20 mM) were taken and added into 3 mL of each receptor solution (10  $\mu\text{M}$ ) prepared above to make 2.0 equiv. Then, 3.0  $\mu\text{L}$  of  $\text{Fe}(\text{ClO}_4)_2$  solution (20 mM) were added into the mixed solution of each metal ion and **1** to make 2.0 equiv. After mixing them for two minutes, UV-vis absorption spectra were taken at room temperature.

For  $\text{Fe}^{3+}$  ion; **1** (3.1 mg, 0.003 mmol) was dissolved in MeOH (2 mL). 10  $\mu\text{L}$  of **1** (3 mM) were diluted with 2.990 mL MeOH-buffer solution (9:1, v/v, 10 mM, bis-tris, pH 7.0) to make the final concentration of 10  $\mu\text{M}$ .  $\text{MNO}_3$  (M = Na, K, 0.02 mmol),  $\text{M}(\text{NO}_3)_2$  (M = Mg, Ca, Mn, Ni, Cu, Zn, Cd, Hg, 0.02 mmol),  $\text{M}(\text{NO}_3)_3$  (M = Al, Cr, Fe, Ga, In, 0.02 mmol) and  $\text{Fe}(\text{ClO}_4)_2$  (15.6 mg, 0.02 mmol) were dissolved in MeOH (3 mL), respectively. 1.8  $\mu\text{L}$  of each metal solution (20 mM) were taken and added into 3 mL of each receptor solution (10  $\mu\text{M}$ ) prepared above to make 1.8 equiv. Then, 3.0  $\mu\text{L}$  of  $\text{Fe}(\text{NO}_3)_3$  solution (20 mM) were added into the mixed solution of each metal ion and **1** to make 1.8 equiv. After mixing them for two minutes, UV-vis absorption spectra were taken at room temperature.

**Job plot measurements.** For  $\text{Fe}^{2+}$ ; Receptor **1** (3.1 mg, 0.003 mmol) was dissolved in MeOH (2 mL). 100, 90, 80, 70, 60, 50, 40, 30, 20, 10 and 0  $\mu\text{L}$  of **1** solution were taken and transferred to vials. Each vial was diluted with MeOH-buffer solution (9:1, v/v, 10 mM, bis-tris, pH 7.0) to make a total volume of 2.9 mL.  $\text{Fe}(\text{ClO}_4)_2$  (2.3 mg, 0.003 mmol) was

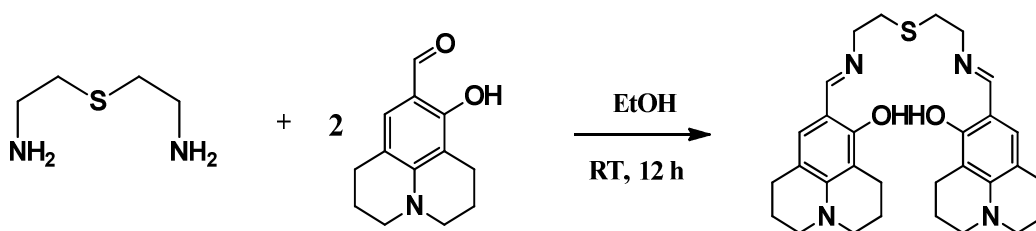
dissolved in MeOH (3 mL). 0, 10, 20, 30, 40, 50, 60, 70, 80, 90, and 100  $\mu\text{L}$  of the  $\text{Fe}^{2+}$  solution were added to each diluted **1** solution. Each vial had a total volume of 3 mL. After shaking them for two minutes, fluorescence spectra were taken at room temperature.

For  $\text{Fe}^{3+}$ ; **1** (3.1 mg, 0.003 mmol) was dissolved in MeOH (2 mL). 100, 90, 80, 70, 60, 50, 40, 30, 20, 10 and 0  $\mu\text{L}$  of **1** solution were taken and transferred to vials. Each vial was diluted with MeOH-buffer solution (9:1, v/v, 10 mM, bis-tris, pH 7.0) to make a total volume of 2.9 mL.  $\text{Fe}(\text{NO}_3)_3$  (3.7 mg, 0.003 mmol) was dissolved in MeOH (3 mL). 0, 10, 20, 30, 40, 50, 60, 70, 80, 90, and 100  $\mu\text{L}$  of the  $\text{Fe}^{3+}$  solution were added to each diluted **1** solution. Each vial had a total volume of 3 mL. After shaking them for two minutes, fluorescence spectra were taken at room temperature.

## Results and discussion

### Synthesis of **1**

A new chemosensor **1** was synthesized by the condensation reaction of 8-hydroxyjulolidine-9-carboxaldehyde with 2,2'-thiobis-(ethylamine) in ethanol at room temperature (Scheme 1), and characterized by  $^1\text{H}$  and  $^{13}\text{C}$  NMR, ESI-mass spectrometry and elemental analysis.



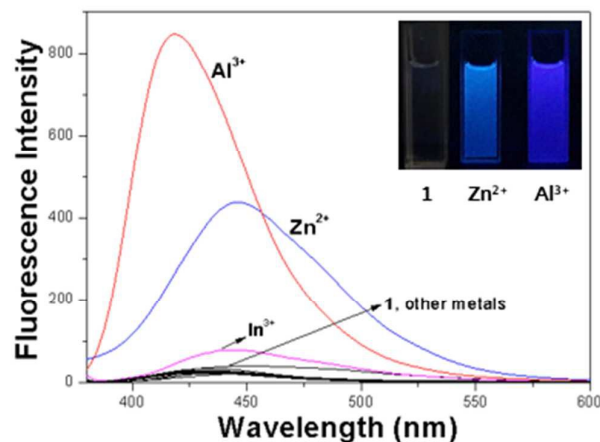
Scheme 1. Synthesis of **1**.

### Fluorogenic sensing for $\text{Zn}^{2+}$ and $\text{Al}^{3+}$ in DMF

The receptor **1** alone has a very weak fluorescence emission with an excitation of 355 nm in DMF. When 11 equiv of various metal ions such as  $\text{Al}^{3+}$ ,  $\text{Ga}^{3+}$ ,  $\text{In}^{3+}$ ,  $\text{Zn}^{2+}$ ,  $\text{Cd}^{2+}$ ,  $\text{Cu}^{2+}$ ,  $\text{Fe}^{2+}$ ,  $\text{Fe}^{3+}$ ,  $\text{Mg}^{2+}$ ,  $\text{Cr}^{3+}$ ,  $\text{Hg}^{2+}$ ,  $\text{Ag}^+$ ,  $\text{Co}^{2+}$ ,  $\text{Ni}^{2+}$ ,  $\text{Na}^+$ ,  $\text{K}^+$ ,  $\text{Ca}^{2+}$ ,  $\text{Mn}^{2+}$  and  $\text{Pb}^{2+}$  were added to **1**, the

solution of **1** exhibited no or slight increase of the fluorescence except  $\text{Zn}^{2+}$  and  $\text{Al}^{3+}$  (Figure 1). The addition of  $\text{Zn}^{2+}$  and  $\text{Al}^{3+}$  resulted in significant enhancements of the emission intensities at 448 nm (32-folds) and 418 nm (35-folds), respectively. These two emissions at different wavelengths indicate that **1** could be used as a dual chemosensor for  $\text{Zn}^{2+}$  and  $\text{Al}^{3+}$  in the same solvent environment.

(a)



(b)

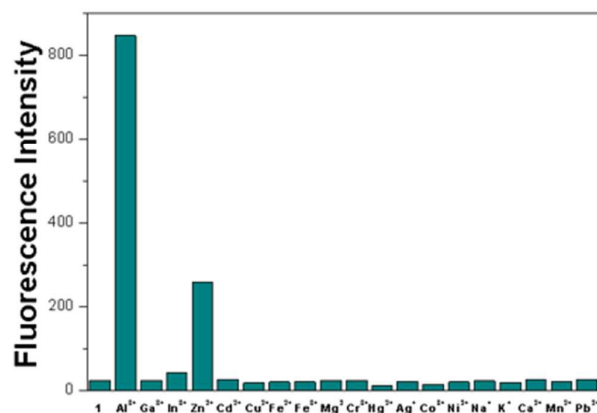
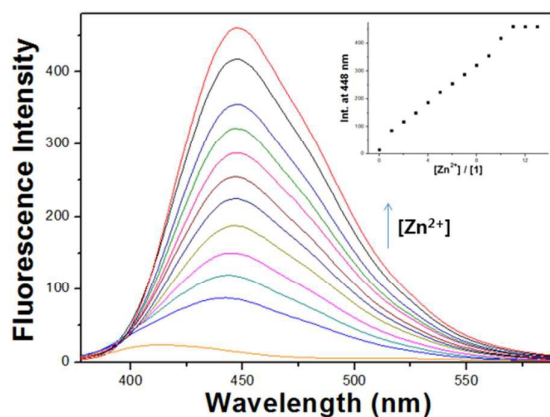


**Figure 1.** (a) Fluorescence spectra of **1** (10  $\mu\text{M}$ ) upon addition of metal salts (9 equiv) of  $\text{Al}^{3+}$ ,  $\text{Ga}^{3+}$ ,  $\text{In}^{3+}$ ,  $\text{Zn}^{2+}$ ,  $\text{Cd}^{2+}$ ,  $\text{Cu}^{2+}$ ,  $\text{Fe}^{2+}$ ,  $\text{Fe}^{3+}$ ,  $\text{Mg}^{2+}$ ,  $\text{Cr}^{3+}$ ,  $\text{Hg}^{2+}$ ,  $\text{Ag}^+$ ,  $\text{Co}^{2+}$ ,  $\text{Ni}^{2+}$ ,  $\text{Na}^+$ ,  $\text{K}^+$ ,  $\text{Ca}^{2+}$ ,  $\text{Mn}^{2+}$  and  $\text{Pb}^{2+}$  in DMF ( $\lambda_{\text{ex}} = 355 \text{ nm}$ ). (b) Bar graph representing the change of the relative emission intensity of **1** at 460 nm upon treatment with various metal ions ( $\lambda_{\text{ex}} = 355 \text{ nm}$ ).

The changes in the emission spectra of **1** as function of the concentration of  $\text{Zn}^{2+}$  and  $\text{Al}^{3+}$  are shown in Figure 2. Upon the addition of  $\text{Zn}^{2+}$ , fluorescence intensity increased gradually and was saturated with 11 equiv of  $\text{Zn}^{2+}$  (Figure 2(a)). When the fluorescent titration was performed with  $\text{Al}^{3+}$ , the emission intensity increased up to 11 equiv and then no further change was observed (Figure 2(b)).

The significant increase of fluorescence by the addition of  $\text{Zn}^{2+}$  and  $\text{Al}^{3+}$  into **1** could be explained by the inhibition of both the C=N isomerization and excited-state proton transfer (ESPT). Imines are generally known to be poorly fluorescent, in part due to isomerization of the C=N double bond in the excited state<sup>46</sup> and in part due to ESPT involving the phenolic protons of the julolidine moiety.<sup>47</sup> Upon stable chelation with a certain metal, the C=N isomerization and ESPT are inhibited (Scheme 2), thus leading to fluorescence enhancement. Also, we consider the chelation-enhanced fluorescence (CHEF) effect as the responsive mechanism for fluorescence enhancements of **1**- $\text{Zn}^{2+}$  complex and **1**- $\text{Al}^{3+}$  complex. The chelating of **1** with  $\text{Zn}^{2+}$  and  $\text{Al}^{3+}$  induced rigidity in the complexes, leading to a large CHEF effect with the drastic enhancement of fluorescence.<sup>48</sup>

(a)



(b)

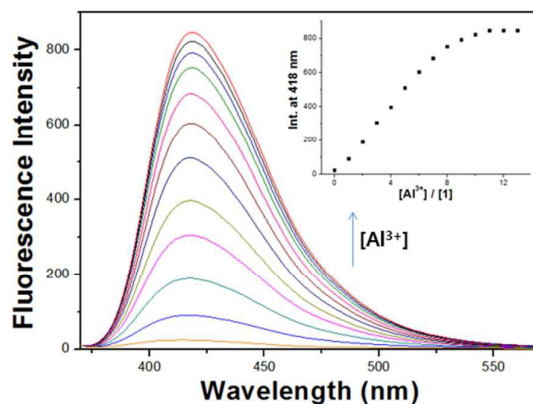
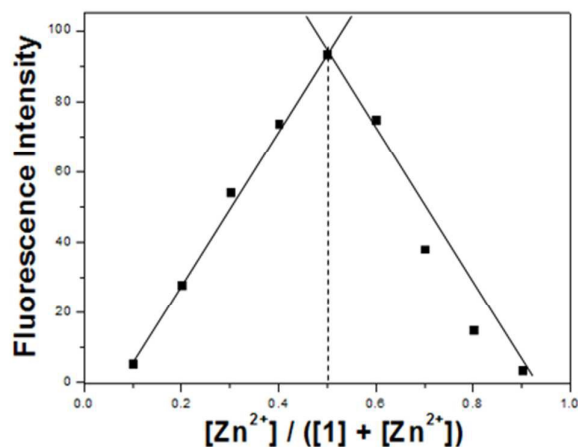


**Figure 2.** (a) Fluorescence spectra of **1** (10  $\mu\text{M}$ ;  $\lambda_{\text{ex}} = 355 \text{ nm}$ ) after addition of increasing amounts of  $\text{Zn}^{2+}$  ions (1, 2, 3, 4, 5, 6, 7, 8, 9, 10, 11, 12 and 13 equiv) at room temperature. Inset: Plot of the fluorescence intensity at 445 nm as a function of  $\text{Zn}^{2+}$  concentration. (b) Fluorescence spectra of **1** (10  $\mu\text{M}$ ;  $\lambda_{\text{ex}} = 355 \text{ nm}$ ) after addition of increasing amounts of  $\text{Al}^{3+}$  ions (1, 2, 3, 4, 5, 6, 7, 8, 9, 10, 11, 12 and 13 equiv) at room temperature. Inset: Plot of the fluorescence intensity at 418 nm as a function of  $\text{Al}^{3+}$  concentration.

To further explore the interaction between **1** and the two metal ions  $\text{Zn}^{2+}$  and  $\text{Al}^{3+}$ , UV-vis titrations were carried out (Figure S1). Upon addition of  $\text{Zn}^{2+}$  ions to a solution of **1**, the absorption band at 351 nm decreased and the absorbance intensity at 374 nm increased with an isosbestic point at 358 nm, which indicates a clean conversion of **1** into the **1**- $\text{Zn}^{2+}$  complex. Similarly, the addition of  $\text{Al}^{3+}$  ion to a solution of **1** resulted in a decrease of absorption peak at 352 nm and appearance of a new peak at 380 nm with a clear isosbestic point at 363 nm, which indicates the clean formation of **1**- $\text{Al}^{3+}$  complex.

The binding modes between **1** and the two metal ions,  $\text{Zn}^{2+}$  and  $\text{Al}^{3+}$ , were determined by using Job plot analysis. As shown in Figure 3, the Job plots for the **1**- $\text{Zn}^{2+}$  and **1**- $\text{Al}^{3+}$  complexes exhibited 1:1 complexation stoichiometry, respectively.

(a)



(b)

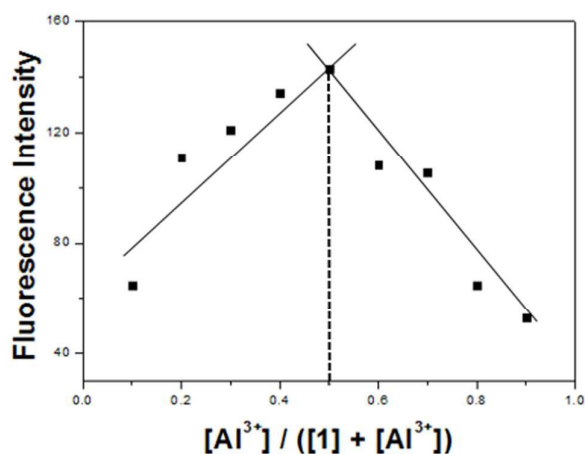


**Figure 3.** Job plots of 1-Zn<sup>2+</sup> and 1-Al<sup>3+</sup> complexes. The total concentration of 1 and metal ions (Zn<sup>2+</sup> and Al<sup>3+</sup>) was 40  $\mu$ M, fluorescence intensity at 449 nm respectively.

From the results of fluorescence titration, the association constants of the 1-Zn<sup>2+</sup> and 1-Al<sup>3+</sup> complexes were determined as  $2.9 \times 10^4 \text{ M}^{-1}$  and  $8.5 \times 10^3 \text{ M}^{-1}$  on the basis of Benesi-Hildebrand equation (Figure S2). These values are comparable to those reported for Zn<sup>2+</sup>-chemosensors ( $10^1 \sim 10^7 \text{ M}^{-1}$ ) and Al<sup>3+</sup>-chemosensors ( $10^3 \sim 10^{14} \text{ M}^{-1}$ ).<sup>47,48</sup> For practical application, the detection limit was also an important parameter. Thus, the detection limits of



protons of the hydroxyl groups at 13.7 ppm disappeared due to their deprotonation, and the H<sub>2</sub> protons of the C=N moieties and the H<sub>4</sub> and H<sub>5</sub> protons of the ethylene moiety were shifted to downfield. These results suggest that the bridge S, the imine N, and the phenol O atoms might coordinate to Zn ion.<sup>50</sup>

<sup>1</sup>H NMR titration experiments of **1** with Al(NO<sub>3</sub>)<sub>3</sub> were also carried out in DMF-*d*<sub>7</sub> (Figure S5). Upon addition of the Al<sup>3+</sup> to **1**, the O-H peaks at 13.6 ppm disappeared completely. In addition, the protons of the imine and ethylene moieties showed a similar pattern as observed in **1**-Zn<sup>2+</sup> complex, demonstrating that both **1**-Al<sup>3+</sup> and **1**-Zn<sup>2+</sup> complexes might have a similar coordination environment.

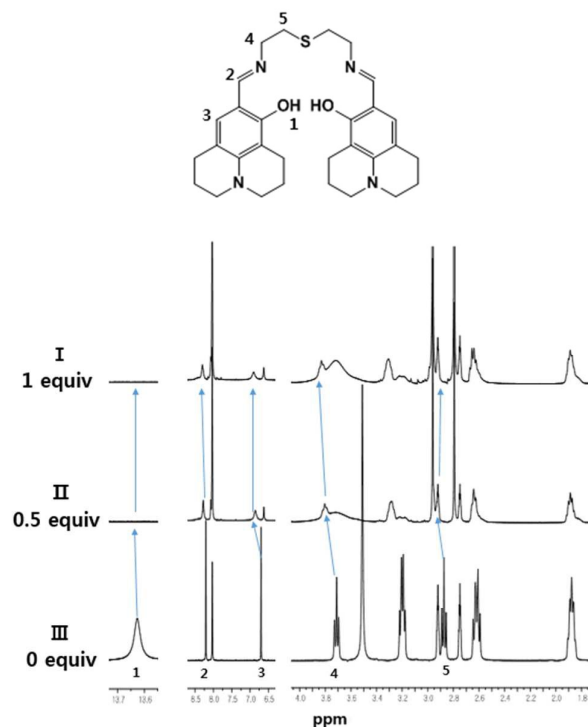
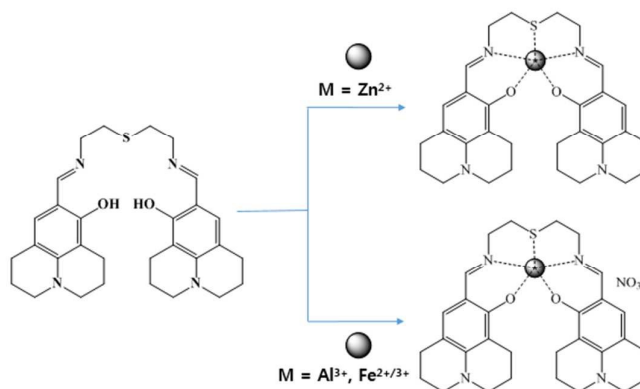


**Figure 5.** (a) <sup>1</sup>H NMR titration of **1** with Zn<sup>2+</sup> in DMF-*d*<sub>7</sub>: (a) only **1**; (b) **1**+Zn<sup>2+</sup> (0.5 equiv); (c) **1**+Zn<sup>2+</sup> (1 equiv).

The formation of **1**-Zn<sup>2+</sup> and **1**-Al<sup>3+</sup> complexes was further confirmed by ESI-mass

spectrometry analysis. The positive-ion mass spectrum of **1** upon addition of 1 equiv of  $\text{Zn}^{2+}$  showed the formation of  $\mathbf{1} + \text{Zn}^{2+} - \text{H}^+$  complex [ $m/z$ : 581.267; calcd ; 581.193] (Figure S6a). For  $\text{Al}^{3+}$ , the positive-ion mass spectrum of **1** showed the formation  $\mathbf{1} + \text{Al}^{3+} - 2\text{H}^+$  complex [ $m/z$ : 543.333; calcd.,: 543.236] (Figure S6b). Based on Job plot,  $^1\text{H}$  NMR titration, and ESI-mass spectrometry analysis, we propose the structures of  $\mathbf{1} - \text{Zn}^{2+}$  and  $\mathbf{1} - \text{Al}^{3+}$  complexes as shown in Scheme 2.

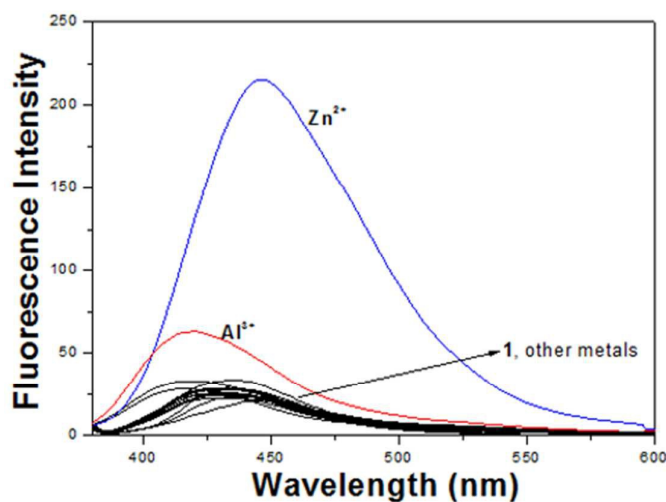


**Scheme 2.** Proposed structures of  $\mathbf{1} - \text{M}^{n+}$  complex.

### Fluorogenic sensing for $\text{Zn}^{2+}$ in aqueous media

For practical application of receptor **1** toward various metal ions, we increased the amount of the bis-tris buffer in DMF. **1** alone displayed a very weak emission band at 440 nm with excitation at 355 nm in DMF-buffer solution (95:5, v/v, 10 mM, bis-tris, pH 7.0) (Figure 6). Upon the addition of various metal ions, the metal ions showed either no or slight change in the emission spectra relative to the free **1** except for  $\text{Ga}^{3+}$ ,  $\text{In}^{3+}$ ,  $\text{Al}^{3+}$  and  $\text{Zn}^{2+}$ . Surprisingly, only  $\text{Zn}^{2+}$  induced a noticeable intensity enhancement among the four metal ions, while the rest three metal ions showed a small increase in the emission spectra. Unlike remarkable fluorescence enhancement for  $\text{Al}^{3+}$  in DMF, slight fluorescence enhancement for  $\text{Al}^{3+}$  in aqueous solution might be due to the weak coordination ability of  $\text{Al}^{3+}$  to **1** by the strong hydrogen bonding between water and a hard acid  $\text{Al}^{3+}$ . These results suggest that **1** could be a good fluorescent chemosensor for  $\text{Zn}^{2+}$  among various metal ions in aqueous solution.<sup>49</sup>

(a)



(b)

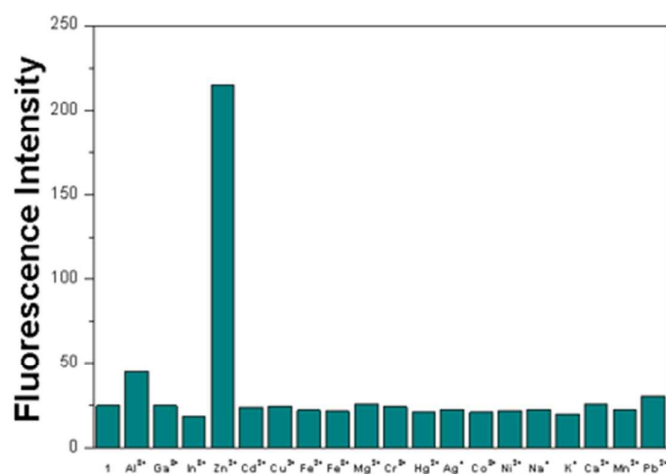


**Figure 6.** (a) Fluorescence spectra of **1** (10  $\mu\text{M}$ ) upon addition of metal salts (10 equiv) of  $\text{Al}^{3+}$ ,  $\text{Ga}^{3+}$ ,  $\text{In}^{3+}$ ,  $\text{Zn}^{2+}$ ,  $\text{Cd}^{2+}$ ,  $\text{Cu}^{2+}$ ,  $\text{Fe}^{2+}$ ,  $\text{Fe}^{3+}$ ,  $\text{Mg}^{2+}$ ,  $\text{Cr}^{3+}$ ,  $\text{Hg}^{2+}$ ,  $\text{Ag}^+$ ,  $\text{Co}^{2+}$ ,  $\text{Ni}^{2+}$ ,  $\text{Na}^+$ ,  $\text{K}^+$ ,  $\text{Ca}^{2+}$ ,  $\text{Mn}^{2+}$  and  $\text{Pb}^{2+}$  in DMF-buffer solution (95:5, v/v, 10 mM, bis-tris, pH 7.0) ( $\lambda_{\text{ex}} = 355 \text{ nm}$ ). (b) Bar graph representing the change of the relative emission intensity of **1** at 460 nm upon treatment with various metal ions ( $\lambda_{\text{ex}} = 355 \text{ nm}$ ).

The fluorescence titration for the binding of **1** with  $\text{Zn}^{2+}$  is shown in Figure 7. The emission intensity of **1** gradually increased with concentration of  $\text{Zn}^{2+}$ , and was saturated at 12 equiv of

Zn<sup>2+</sup>.

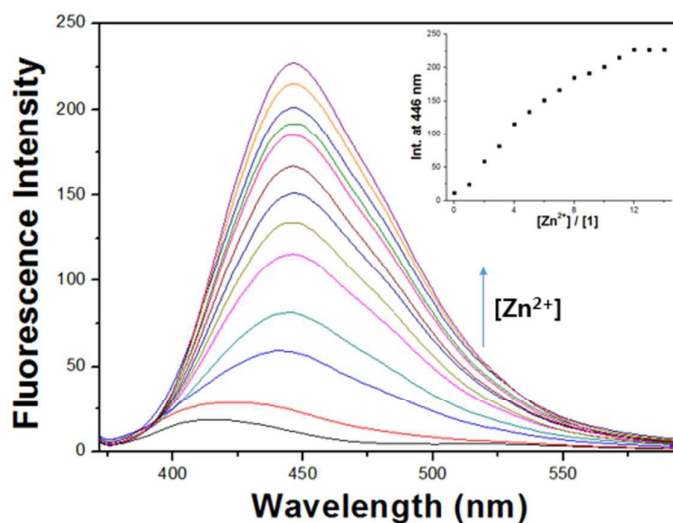


**Figure 7.** Fluorescence spectra of **1** (10  $\mu\text{M}$ ;  $\lambda_{\text{ex}} = 355 \text{ nm}$ ) after addition of increasing amounts of  $\text{Zn}^{2+}$  ions (1, 2, 3, 4, 5, 6, 7, 8, 9, 10, 11, 12 and 13 equiv) in the DMF-buffer solution (95:5, v/v, 10 mM bis-tris, pH 7.0) at room temperature. Inset: Plot of the fluorescence intensity at 446 nm as a function of  $\text{Zn}^{2+}$  concentration.

The Job plot showed 1:1 complexation of **1** and  $\text{Zn}^{2+}$  (Figure 8). From the fluorescence titration, the association constant was calculated to be  $7.7 \times 10^3 \text{ M}^{-1}$  by Benesi-Hildebrand equation (Figure S7). This value is lower than that obtained in DMF, suggesting that water might interfere somewhat with the complexation of **1** and  $\text{Zn}^{2+}$  through the hydrogen bonding. The detection limit of **1** as a fluorescence chemosensor for analysis of  $\text{Zn}^{2+}$  was found to be  $3.74 \mu\text{M}$  using of the basis  $3\sigma/K$  (Figure S8),<sup>33</sup> which is far below the World Health Organization guideline ( $76 \mu\text{M}$ ). This result indicates that **1** could be an influential device for the detection of zinc in the drinking water.

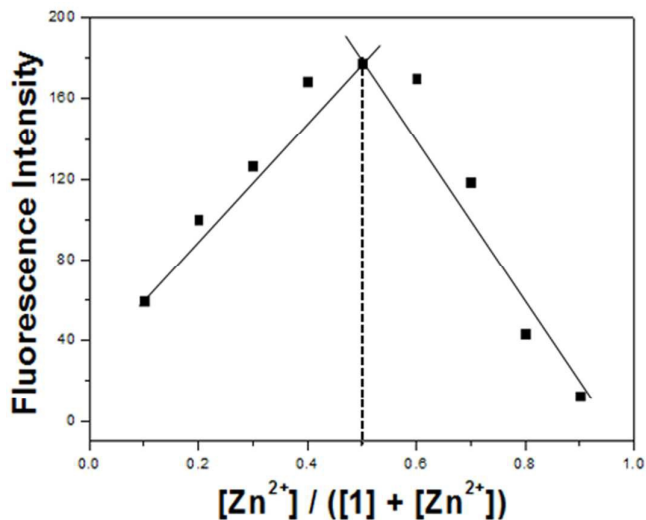


**Figure 8.** Job plot of **1** and Zn<sup>2+</sup> in DMF-buffer solution (95:5, v/v, 10 mM, bis-tris, pH 7.0). The total concentration of **1** and Zn<sup>2+</sup> was 40  $\mu$ M (fluorescence intensity at 430 nm).

To further check the practical applicability of **1** as Zn<sup>2+</sup> selective fluorescent sensor, we carried out competition experiments in the presence of various metal ions (Figure S9). When **1** was treated with 12 equiv of Zn<sup>2+</sup> in the presence of the same concentration of other metal ions (Al<sup>3+</sup>, Ga<sup>3+</sup>, In<sup>3+</sup>, Cd<sup>2+</sup>, Cu<sup>2+</sup>, Fe<sup>2+</sup>, Fe<sup>3+</sup>, Mg<sup>2+</sup>, Cr<sup>3+</sup>, Hg<sup>2+</sup>, Ag<sup>+</sup>, Co<sup>2+</sup>, Ni<sup>2+</sup>, Na<sup>+</sup>, K<sup>+</sup>, Mn<sup>2+</sup>, Ca<sup>2+</sup> and Pb<sup>2+</sup>), Al<sup>3+</sup>, Fe<sup>3+</sup>, Cr<sup>3+</sup> and Co<sup>2+</sup> ions inhibited about 70% of the interaction between **1** and Fe<sup>2+</sup> and Cu<sup>2+</sup> did completely.

To examine the reversibility of **1** toward Zn<sup>2+</sup> in DMF-buffer solution (95:5, v/v, 10 mM, bis-tris, pH 7.0), EDTA was added to the mixed solution of **1** and Zn<sup>2+</sup> (Figure S10). The solution of **1**-Zn<sup>2+</sup> complex resulted in the disappearance of its emission intensity, which indicates the regeneration of the free **1**. Upon addition of Zn<sup>2+</sup> into the mixture solution again, the fluorescence intensity was recovered to original intensity of **1**-Zn<sup>2+</sup> complex. These results indicate that **1** could be recyclable through treatment with a proper reagent such as EDTA.

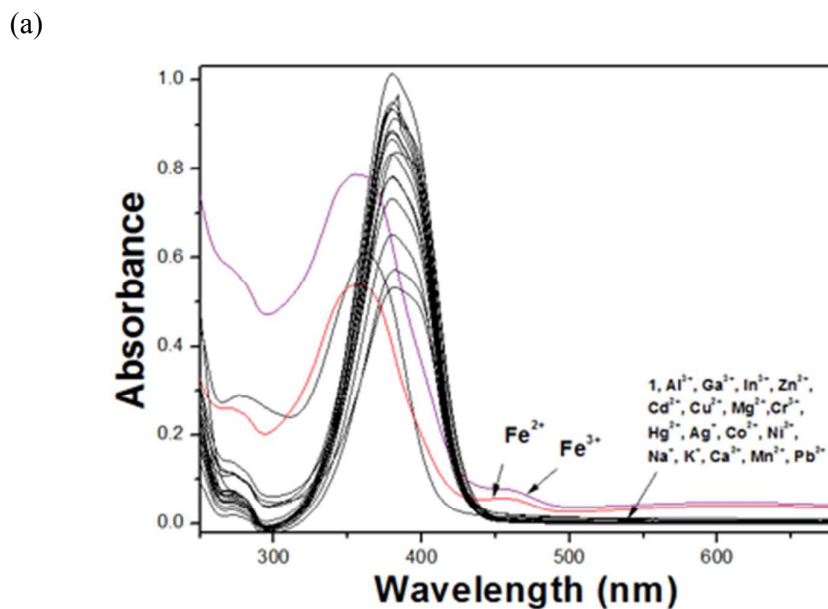
We also constructed the calibration curve for the determination of Zn<sup>2+</sup> by **1** (Figure S11). Receptor **1** exhibited a good linear relationship between the fluorescence intensity of **1** and Zn<sup>2+</sup> concentration (0.00-120.00  $\mu$ M) with correlation coefficient of  $R^2 = 0.9982$  ( $n = 3$ ),

which means that **1** is suitable for quantitative detection of  $\text{Zn}^{2+}$ . In order to examine the applicability of the chemosensor **1** in environmental samples, **1** was applied to the determination of  $\text{Zn}^{2+}$  in a tap water sample by using the calibration curve. As shown in Table S1, one can see that the satisfactory recovery and R.S.D. values of the tap water sample were exhibited.

### Chromogenic sensing for $\text{Fe}^{2+}$ and $\text{Fe}^{3+}$ in aqueous solution

The chromogenic sensing ability of **1** was examined with nitrate salt of various metal ions such as  $\text{Al}^{3+}$ ,  $\text{Ga}^{3+}$ ,  $\text{In}^{3+}$ ,  $\text{Zn}^{2+}$ ,  $\text{Cd}^{2+}$ ,  $\text{Fe}^{2+}$ ,  $\text{Fe}^{3+}$ ,  $\text{Mg}^{2+}$ ,  $\text{Cr}^{3+}$ ,  $\text{Hg}^{2+}$ ,  $\text{Ag}^+$ ,  $\text{Co}^{2+}$ ,  $\text{Ni}^{2+}$ ,  $\text{Na}^+$ ,  $\text{K}^+$ ,  $\text{Ca}^{2+}$ ,  $\text{Mn}^{2+}$ ,  $\text{Pb}^{2+}$  and  $\text{Cu}^{2+}$  in MeOH-buffer solution (9:1, v/v, 10 mM, bis-tris, pH 7.0) at room temperature. As shown in Figure 9, both  $\text{Fe}^{2+}$  and  $\text{Fe}^{3+}$  ion induced distinct spectral and instant color changes from pale yellow to dark green, while other metal ions did not produce any change. This result indicates that **1** could be used as a “naked-eye” sensor for  $\text{Fe}^{2+}$  and  $\text{Fe}^{3+}$  ion in aqueous media. These peaks with molar extinction coefficients in the thousands,  $8.0 \times 10^3 \text{ M}^{-1}\text{cm}^{-1}$  ( $\epsilon_{455\text{nm}}$ ) for  $\text{Fe}^{2+}$  and  $7.8 \times 10^3 \text{ M}^{-1}\text{cm}^{-1}$  ( $\epsilon_{455\text{nm}}$ ) for  $\text{Fe}^{3+}$ , are too large to be Fe-based d-d transitions. Thus, these new peaks might be attributed to a metal-to-ligand charge-transfer (MLCT),<sup>51</sup> which is responsible for the dark green color of the solutions.

On the other hand,  $\text{Zn}^{2+}$  and  $\text{Al}^{3+}$  ions showed the enhanced fluorescence by the complexations of **1** with them in DMF. These results led us to figure out UV-vis spectral changes of **1** with the two metal ions  $\text{Zn}^{2+}$  and  $\text{Al}^{3+}$  in MeOH-buffer solution (9:1, v/v, 10 mM, bis-tris, pH 7.0). The UV-vis titration experiments for **1**- $\text{Zn}^{2+}$  and **1**- $\text{Al}^{3+}$  species showed no absorbance in the visible light region (Figure S12), indicating no color changes for them. These results suggest that although **1**- $\text{Zn}^{2+}$  and **1**- $\text{Al}^{3+}$  complexes form by the reaction of **1** with the two metal ions  $\text{Zn}^{2+}$  and  $\text{Al}^{3+}$ , they do not have color in MeOH-buffer solution (9:1, v/v, 10 mM, bis-tris, pH 7.0).



(b)

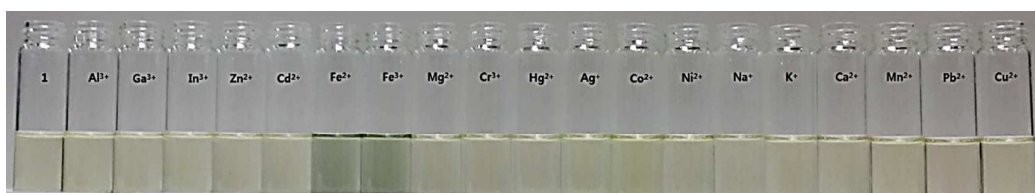


**Figure 9.** (a) UV-vis absorption spectra of **1** (10  $\mu\text{M}$ ) in the presence of 2 equiv of different metal ions in MeOH-buffer solution (9:1, v/v, 10 mM, bis-tris, pH 7.0). (b) Color change of **1** (30  $\mu\text{M}$ ) in the presence of 2 equiv of different metal ions.

In order to understand the binding properties between **1** and  $\text{Fe}^{2+}$  and  $\text{Fe}^{3+}$  ions, the UV-vis titration experiments were carried out (Figure 10). Upon the addition of  $\text{Fe}^{2+}$  ion to **1** solution, the absorbance at 456 nm increased while the absorption peak at 378 nm decreased with isosbestic points at 363 nm and 429 nm. The two clear isosbestic points indicate the clean formation of **1**- $\text{Fe}^{2+}$  complex. **1**- $\text{Fe}^{3+}$  complex also showed almost identical UV-vis variation with **1**- $\text{Fe}^{2+}$ .

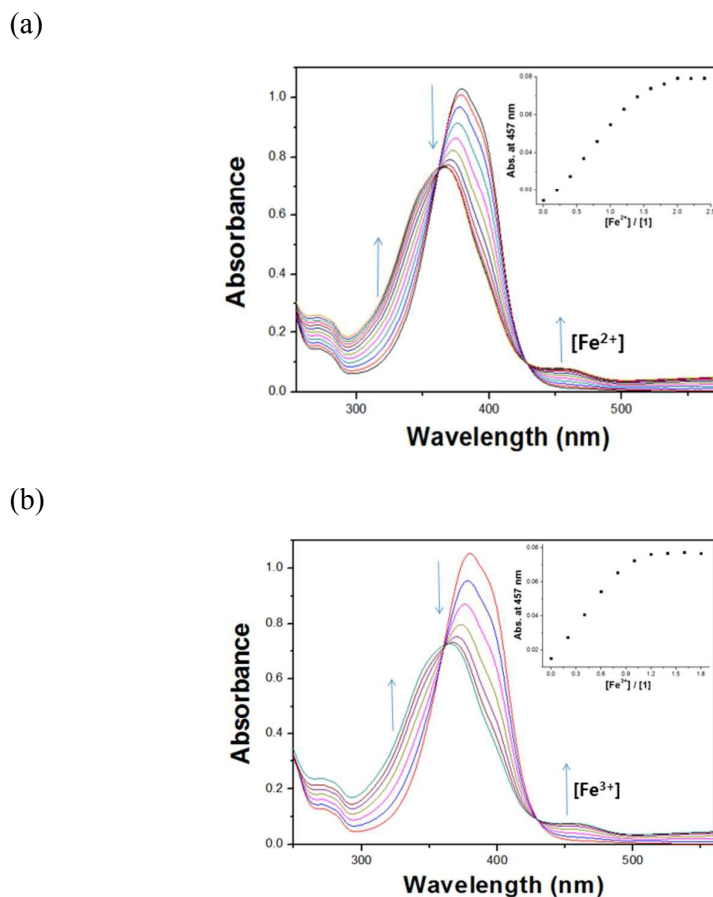
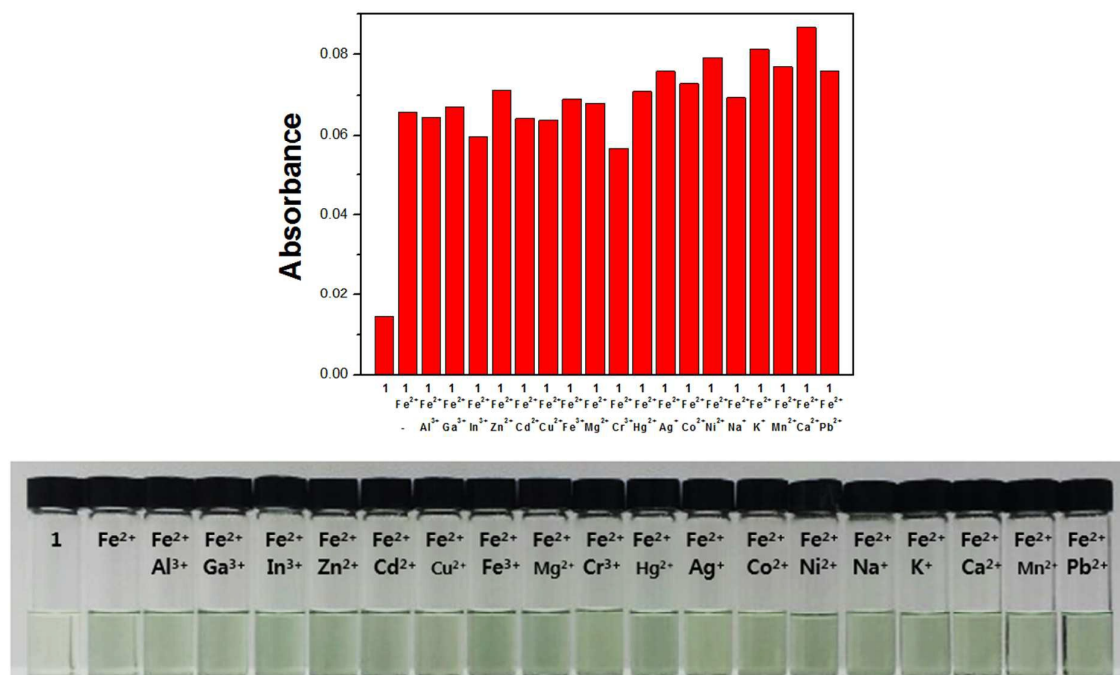


**Figure 10.** (a) UV-vis spectra of **1** (10  $\mu\text{M}$ ) upon the addition of increasing amounts of  $\text{Fe}^{2+}$ . Inset: Plot of the UV-vis absorbance at 457 nm as a function of  $\text{Fe}^{2+}$  concentration. (b) UV-vis spectra of **1** (10  $\mu\text{M}$ ) upon the addition of increasing amounts of  $\text{Fe}^{3+}$ . Inset: Plot of the UV-vis absorbance at 457 nm as a function of  $\text{Fe}^{3+}$  concentration.

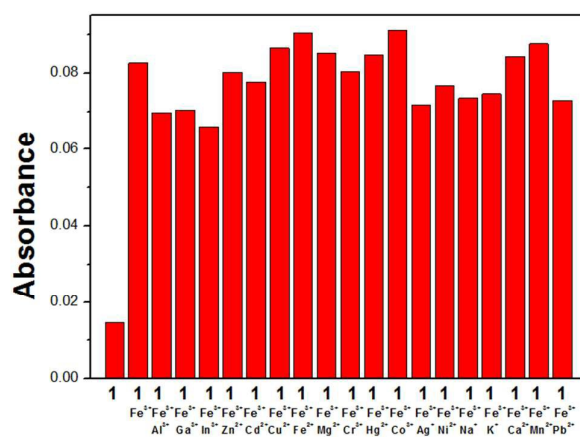
Job plot analysis exhibited 1:1 complexation stoichiometries for **1**- $\text{Fe}^{2+}$  and **1**- $\text{Fe}^{3+}$  complex formations (Figure S13), which were further confirmed by ESI-mass spectrometry analysis (Figure S14). The positive-ion mass spectrum of **1** upon addition of 1 equiv of  $\text{Fe}^{3+}$  showed the formation of **1** -2  $\text{H}^+$  +  $\text{Fe}^{3+}$  complex [ $m/z$ : 572.267; calcd, 572.191]. In case of  $\text{Fe}^{2+}$ , the formation of **1**- $\text{Fe}^{3+}$  complex was observed [**1** -2  $\text{H}^+$  +  $\text{Fe}^{3+}$ ;  $m/z$ : 572.200; calcd, 572.191], even though  $\text{Fe}^{2+}$  was used as the standard metal ion. This phenomenon could be explained by one of two possibilities: the one is that the **1**- $\text{Fe}^{2+}$  complex might be oxidized to the **1**- $\text{Fe}^{3+}$  complex under ESI-mass experimental conditions, and the other is that after its formation

from the reaction of  $\text{Fe}^{2+}$  with **1**, the  $\mathbf{1}\text{-Fe}^{2+}$  complex is oxidized to the  $\mathbf{1}\text{-Fe}^{3+}$  complex. Nearly identical UV-vis titration experiments of  $\mathbf{1}\text{-Fe}^{2+}$  and  $\mathbf{1}\text{-Fe}^{3+}$  complexes (Figure 10) suggest that the latter would happen. Based on Job plot and ESI-mass spectrometry analysis, we propose the structures of  $\mathbf{1}\text{-Fe}^{2+}$  and  $\mathbf{1}\text{-Fe}^{3+}$  complexes as shown in Scheme 2.

(a)



(b)



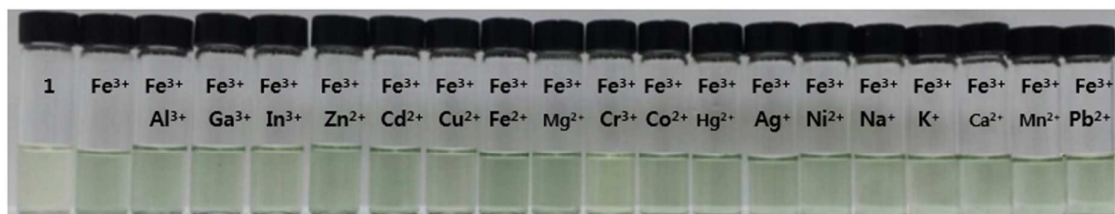


**Figure 11.** (a) Effect of competitive metal ions (20  $\mu\text{M}$ ) on the interaction between **1** (10  $\mu\text{M}$ ) and  $\text{Fe}^{2+}$  ion (20  $\mu\text{M}$ ) (UV-vis absorbance at 450 nm). (b) Effect of competitive metal ions (12  $\mu\text{M}$ ) on the interaction between **1** (10  $\mu\text{M}$ ) and  $\text{Fe}^{3+}$  ion (12  $\mu\text{M}$ ) (UV-vis absorbance at 450 nm).

The binding constants ( $K$ ) of **1** with  $\text{Fe}^{2+}$  and  $\text{Fe}^{3+}$  were calculated as  $1.1 \times 10^4$  and  $1.2 \times 10^4$  on the basis of Benesi-Hildebrand analysis, respectively (Figure S15). These values are the range  $10^4$ - $10^5$  and  $10^3$ - $10^5$  of those previously reported for  $\text{Fe}^{2+}$  and  $\text{Fe}^{3+}$  binding sensors, respectively. The absorption titration profiles of **1** with  $\text{Fe}^{2+}$  and  $\text{Fe}^{3+}$  demonstrated that the detection limits of  $\text{Fe}^{2+}$  and  $\text{Fe}^{3+}$  were 0.21  $\mu\text{M}$  and 0.22  $\mu\text{M}$  using of the basis  $3\sigma/K$  (Figure S16) [43]. WHO recommends that the acceptable limit for iron in drinking water would be 5.36  $\mu\text{M}$  [44].

The UV-vis competitive studies of **1** with  $\text{Fe}^{2+}$  and  $\text{Fe}^{3+}$  were investigated in the presence of other metal ions (Figure 11). A background of most competing metal ions did not interfere with the detection of  $\text{Fe}^{2+}$  and  $\text{Fe}^{3+}$  by **1**.

We also constructed the calibration curve for the determination of  $\text{Fe}^{3+}$  by **1** (Figure S17). Receptor **1** exhibited a good linear relationship between the UV-vis spectra of **1** and  $\text{Fe}^{3+}$  concentration (0.00-15.00  $\mu\text{M}$ ) with correlation coefficient of  $R^2 = 0.9925$  ( $n = 3$ ), which means that **1** is suitable for quantitative detection of  $\text{Fe}^{3+}$ . In order to examine the applicability of **1** in environmental samples, we carried out the determination of  $\text{Fe}^{3+}$  by using the calibration curve in water samples. First, tap water samples were chosen. As shown in Table S2, one can see that the satisfactory recovery and R.S.D. values of water sample was exhibited. Next, we prepared an artificial polluted water sample by adding various metal ions known as being involved in industrial processes into deionized water. The result was also summarized in Table S2, which exhibited the satisfactory recovery and R.S.D. values for the

water sample.

## Conclusions

We have presented a simple, selective and efficient Schiff base chemosensor **1** for  $\text{Zn}^{2+}$  and  $\text{Al}^{3+}$  by fluorescence emission spectra and for  $\text{Fe}^{2+}$  and  $\text{Fe}^{3+}$  by UV-vis spectra. The addition of  $\text{Zn}^{2+}$  and  $\text{Al}^{3+}$  into **1** showed drastic enhancements of the emission intensities in the different wavelength, which means that **1** could be used a dual-sensor in DMF. Also, **1** showed a superb selectivity toward only  $\text{Zn}^{2+}$  over competing relevant metal ions in aqueous media. Moreover, **1** could function as a colorimetric sensor for both Fe(II) and Fe(III) with the color changes from pale yellow to dark green. Importantly, any interference was not observed for the detection of both Fe(II) and Fe(III) in the presence of other metal ions. Therefore, we believe that this highly selective fluorescent and chromogenic sensor would be a good guidance to the development of chemosensors for multiple targets.

## Acknowledgements

Financial support from Basic Science Research Program through the National Research Foundation of Korea (NRF) funded by the Ministry of Education, Science and Technology (2012001725 and 2012008875) are gratefully acknowledged.

## Supplementary Material

Additional experimental data are available. Supplementary data to this article can be found online at doi:10.1016/j.inoche.2014.???.???

## References

1. J. M. Berg and Y. Shi, *Science*, 1996, **271**, 1081-1085.
2. D.W. Choi, J.Y. Koh, *Annurev-neuro.*, 1998, **21**, 347-375.
3. C. J. Frederickson and A. I. Bush, *BioMetals*, 2001, **14**, 353-366.
4. P.D. Zalewski, I.J. Forbes, W.H. Betts, *Biochem. J.*, 1993, **296**, 403-408.
5. K. Falchuk, *Mol. Cell. Biochem.*, 1998, **188**, 41-48.
6. B.L. Vallee, K.H. Falchuk, *Phys. Rev.* 1993, **73**, 79-118.
7. W. Maret, C. Jacob, B.L. Vallee, E.H. Fischer, *Proceedings of the National.*, 1999, **96**, 1910-1914.
8. T. O'Halloran, *Science*, 1993, **261**, 715-725.
9. J.J.R. Fraústo da Silva, R.J.P. Williams, Oxford University Press, Oxford, 1991.
10. M.S. Nasir, C.J. Fahrni, D.A. Suhy, K.J. Kolodnick, C.P. Singer, T.V. O'Halloran, *J. Biol. Inorg. Chem.* 1999, **4**, 775-783.
11. Sougata Sinha, Trinetra Mukherjee, Jomon Mathew, Subhra K. Mukhopadhyay, Subrata Ghosh, *Anal. Chim. Acta*, 2014, **822**, 60-68.
12. F. Qian, C. Zhang, Y. Zhang, W. He, X. Gao, P. Hu, Z. Guo, *J. Am. Chem. Soc.* 2009, **131**, 1460-1468.
13. W. Maret, *Biometals*, 2001, **14**, 187-190.
14. J. Kim, I. Hwang, S. Jang, J. Kang, S. Kim, I. Noh, Y. Kim, C. Kim, R. G. Harrison, *Dalton Trans.*, 2013, **42**, 5500-5507.
15. H. Lee, J. Lee, S. Jang, H. Park, S. Kim, Y. Kim, C. Kim, R. G. Harrison, *Tetrahedron*, 2011, **67**, 8073-8078.
16. K. B. Kim, H. Kim, E. J. Song, S. Kim, I. Noh, C. Kim, *Dalton Trans.*, 2013, **42**, 16569-16577.
17. J. Y. Choi, Dabin Kim, Juyoung Yoon, *Dyes Pigm.*, 2013, **96**, 176-179.
18. H. Lee, J. Lee, S. Jang, I. Hwang, S. Kim, Y. Kim, C. Kim, R. G. Harrison, *Inorg. Chim. Acta*, 2013, **394**, 542-551.
19. A. Truong-Tran, J. Carter, R. Ruffin and P. Zalewski, *BioMetals*, 2001, **14**, 315-330.
20. L. Xue, C. Liu and H. Jiang, *Org. Lett.*, 2009, **11**, 1655-1658.
21. L. Xue, C. Liu and H. Jiang, *Org. Lett.*, 2009, **11**, 3454-3457.

22. J. H. Kim, J. Y. Noh, I. H. Hwang, J. Kang, J. Kim, C. Kim, *Tetrahedron Lett.*, 2013, **54**, 2415-2418.
23. P. Jiang, L. Chen, J. Lin, Q. Liu, J. Ding, X. Gao, Z. Guo, *Chem. Commun.*, 2002, 1424-1425.
24. (a) S. Goswami, S. Paul, A. Manna, *RSC Adv.*, 2013, **3**, 10639-10643; (b) A. Sahana, A. Benerjee, S. Lohar, A. Banik, S. K. Mukhopadhyay, D. A. Safin, M. G. Babashkina, M. Bolte, Y. Garcia, D. Das, *Dalton Trans.*, **42** (2013) 13311-13314.
25. D. Karak, S. Lohar, A. Sahana, S. Guha, A. Banerjee, D. Das, *Anal. Methods*, 2012, **4**, 1906-1908.
26. G. D. Fasman, *Chem. Rev.*, 1996, **149**, 125-165.
27. P. Nayak, *Environ. Res.*, 2002, **89**, 101-115.
28. T. P. Flaten, *Brain Res. Bull.*, 2001, **55**, 187-196.
29. C. N. Martyn, C. Osmond, J. A. Edwardson, D. J. P. Barker, E. C. Harris, R. F. Lacey, *Lancet*, 1989, **333**, 61-62.
30. J. Savory, O. Ghribi, M.S. Forbes, M.M. Herman, *J. Inorg. Biochem.*, 2001, **87**, 15-19.
31. J. R. Walton, *Neurotoxicology*, 2006, **27**, 385-394.
32. J. Croom, I.L. Taylor, *J. Inorg. Biochem.*, 2001, **87**, 51-56.
33. J. S. Perlmutter, L.W. Tempel, K.J. Black, D. Parkinson, R.D. Todd, *Neurology*, 1997, **49**, 1432-1438.
34. K. Soroka, R. S. Vithanage, D. A. Philips, B. Walker, P. K. Dasgupta, *Anal. Chem.*, 1987, **59**, 629-636.
35. P. Aisen, M. Wessling-Resnick, E. A. Leibold, *Curr. Opin. Chem. Biol.*, 1999, **3**, 200-206.
36. E. Beutler, V. Felitti, T. Gelbart, N. Ho, *Drug Metab. Dispos.*, 2001, **29**, 495-499.
37. D. Touati, *Arch. Biochem. Biophys.*, 2000, **373**, 1-6.
38. C. Brugnara, *Clin. Chem.*, 2003, **49**, 1573-1578.
39. Chun-Yan Li, Chun-Xiang Zou, Yong-Fei Li, Jia-Liang Tang, Chao Weng, *Dyes Pigm.*, 2014, **104**, 110-115.
40. P. N. Basa, A. G. Sykes, *J. Org. Chem.*, 2012, **77**, 8428-8434.

41. H. J. Jung, N. Singh, D. Y. Lee, D. O. Jang, *Tetrahedron Lett.*, 2010, **51**, 3962-3965.
42. A. Liu, L. Yang, Z. Zhang, Z. Zhang, D. Xu, *Dyes Pigm.*, 2013, **99**, 472-479.
43. L. wang, H. Li, D. Cao, *Sens. Actuators B*, 2013, **181**, 749-755.
44. M. wang, J. wang, W. xue, A. Wu, *Dyes Pigm.*, 2013, **97**, 475-480.
45. D. Maity, A. K. Manna, D. Karthigeyan, T. K. Kundu, S. K. Pati, T. Govindaraju, *Chem. Eur. J.* 2011, **17**, 11152-11161.
46. G. Q. Yang, F. Morlet-Savary, Z. K. Peng, S. K. Wu, J. P. Fouassier, *Chem. Phys. Lett.*, 1996, **256**, 536-542.
47. M. Royzen, A. Durandin, V. G. Young, N. E. Geacintov, J. W. Canary, *J. Am. Chem. Soc.*, 2006, **128**, 3854-3855.
48. L. Wang, W. Qin, X. Tang, W. Dou, W. Liu, *J. Phys. Chem. A*, 2011, **115**, 1609-1616.
49. Z. Xu, J. Yoon, D. R. Spring, *Chem. Soc. Rev.*, 2010, **39**, 1996-2006.
50. B. N. Ahamed, I. Ravikumar, P. Ghosh, *New J. Chem.*, 2009, **33**, 1825-1828.
51. A. Vogler, H. Kunkely, *Chem. Rev.*, 2000, **208**, 321-329.